Journal of Neuroscience Methods 150 (2006) 265–271

JOURNAL OF NEUROSCIENCE METHODS

www.elsevier.com/locate/jneumeth

Mitochondrial DNA depletion analysis by pseudogene ratioing

Russell H. Swerdlow [a,*], Gerard T. Redpath [b], Daniel R. Binder [a], John N. Davis II [a], Scott R. VandenBerg [c]

[a] *Department of Neurology, University of Virginia Health System, Box 394, Charlottesville, VA 22908, USA*
[b] *Department of Pathology, University of Virginia Health System, Charlottesville, VA 22908, USA*
[c] *Departments of Pathology and Neurological Surgery, University of California, San Francisco, CA, USA*

Received 9 March 2005; received in revised form 21 June 2005; accepted 28 June 2005

Abstract

The mitochondrial DNA (mtDNA) depletion status of ρ^0 cell lines is typically assessed by hybridization or polymerase chain reaction (PCR) experiments, in which the failure to hybridize mtDNA or amplify mtDNA using mtDNA-directed primers suggests thorough mitochondrial genome removal. Here, we report the use of an mtDNA pseudogene ratioing technique for the additional confirmation of ρ^0 status. Total genomic DNA from a U251 human glioma cell line treated with ethidium bromide was amplified using primers designed to anneal either mtDNA or a previously described nuclear DNA-embedded mtDNA pseudogene (mtDNAψ). The resultant PCR product was used to generate plasmid clones. Sixty-two plasmid clones were genotyped, and all arose from mtDNAψ template. These data allowed us to determine with 95% confidence that the resultant mtDNA-depleted cell line contains less than one copy of mtDNA per 10 cells. Unlike previous hybridization or PCR-based analyses of mtDNA depletion, this mtDNAψ ratioing technique does not rely on interpretation of a negative result, and may prove useful as an adjunct for the determination of ρ^0 status or mtDNA copy number.

Keywords: Cybrids; Mitochondrial DNA; Numt; Pseudogene; Rho; U251 cells

1. Introduction

The cytoplasmic hybrid (cybrid) technique of King and Attardi (1989, 1996a) helps evaluate mitochondrial DNA (mtDNA) genotype–phenotype correlations. Cybrids are created through the transfer of mitochondrial DNA (mtDNA) molecules to cultureable cells previously depleted of endogenous mtDNA. Cell lines rendered free of "detectable" mtDNA for such experiments are termed ρ^0 cells (Desjardins et al., 1986).

No universally agreed upon method for screening residual mtDNA in ρ^0 cell lines exists (King and Attardi, 1996b). For the various human ρ^0 cell lines described in the literature, ρ^0 status was determined several different ways. The 143B osteosarcoma ρ^0 cell line described by King and Attardi (1989) was initially characterized by dot–blot hybridization and its inability to survive culture medium not supplemented with pyruvate and uridine. The HeLa cervical carcinoma ρ^0 cell line of Hayashi et al. (1991) was verified by Southern blot hybridization. Demonstration of A549.B2 lung carcinoma ρ^0 cell line status came from Southern blot hybridization and PCR analysis (Bodnar et al., 1993). Lymphoblast ρ^0 cell line reports cite supportive Southern blot hybridization and/or PCR data (Martinus et al., 1993; Trounce et al., 1994). Slot–blot hybridization and oxygen electrode data supported the creation of the SH-SY5Y neuroblastoma ρ^0 cell line (Miller et al., 1996), while cytochrome oxidase activity assay and cell selection in pyruvate/uridine-unsupplemented medium defined the NT2 teratocarcinoma ρ^0 cell line (Swerdlow et al., 1997). A recently described mtDNA in situ fluorescence assay also appears useful for the determination of ρ^0 status (Ashley et al., 2005). Each technique, though, requires interpretation of a negative result, and

* Corresponding author. Tel.: +1 804 924 5785; fax: +1 804 982 1726.
E-mail address: rhs7e@virginia.edu (R.H. Swerdlow).

0165-0270/$ – see front matter © 2005 Elsevier B.V. All rights reserved.
doi:10.1016/j.jneumeth.2005.06.023

mtDNA detection sensitivity may vary substantially between assay types.

To facilitate the assessment of ρ^0 status in mtDNA-depleted cell lines, we now describe a nuclear mtDNA pseudogene (mtDNAψ)–mtDNA ratioing technique. This technique permits the statistical determination of how thorough mtDNA removal is for a particular cell line, and is not dependent upon interpretation of negative results.

2. Materials and methods

2.1. Tissue culture and genomic DNA extraction

U251 glioma cells were grown at 37 °C, 5% CO_2 in tissue culture flasks containing MEM (alpha modification) medium (Hyclone, Logan, UT) supplemented with 10% heat-inactivated fetal bovine serum, 200 μg/ml sodium pyruvate and 200 μg/ml uridine, and with or without ethidium bromide (EtBr). The concentration of EtBr used was determined by trial and error, and represented the maximum amount in which normal cell morphology was maintained. EtBr concentrations varied over the course of these experiments. Cells were harvested with trypsin–EDTA (Gibco BRL, Gaithersburg, MD).

Genomic DNA was extracted with a QIAamp DNA Mini Kit (Qiagen, Valencia, CA) according to the manufacturer's instructions. Aliquots of 5×10^6 cells yielded 5–7 μg of genomic DNA using this method.

2.2. Genomic DNA and nested PCR amplifications

Expand Long Template PCR kits (Roche Diagnostics, Indianapolis, IN) and a GeneAmp 9600 PCR System (PE Biosystems, Foster City, CA) were used for all amplifications. PCR primers that avoid amplification of mtDNAψ sequences present on an extended nuclear-embedded mitochondrial DNA-like sequence (numt) that includes *ND2* through *CO2* homologs were designated $numt_{exclusive}$ primers. Their sequences were as follows: 5′-TGATTTATCTCTC-CACACTAGCAGAGACCAAC-3′ (upper primer; Cambridge sequence nucleotides 3859–3888) and 5′-GCTACA-AAAAATGTTGAGCCGTAGATG-3′ (lower primer; Cambridge sequence nucleotides 9779–9805). For a PCR capable of amplifying either numt DNA or authentic mtDNA, we designed primers complementary to both authentic mtDNA and the ends of the *ND2–CO2* numt. We called these primers $numt_{inclusive}$ primers, and their sequences were as follows: 5′-GAGTCCGAACTAGTCTCAGGCT-3′ (upper primer; Cambridge sequence nucleotides 3916–3937) and 5′-CTCGAAGTACTCTGAGGCTTGTAGGAGG-3′ (lower primer; Cambridge sequence nucleotides 9728–9755). The annealing temperature for both of these reactions was 57.3 °C. The initial extension time was 4 min, which was maintained for the first 10 cycles. Extension times for cycles 11–30 were incrementally increased by 20 s each cycle as per the manufacturer's instructions. The primers for the nested *CO2* amplification were 5′-GCTA-CTTCCCCTATCATAGAAG-3′ (upper primer; Cambridge sequence nucleotides 7619–7640) and 5′-GGGAATTAA-TTCTAGGACGATG-3′ (lower primer; Cambridge sequence nucleotides 8208–8230). This reaction utilized an annealing temperature of 53.6 °C. Reaction products were visualized with UV light following electrophoresis in EtBr gels containing either 1% agarose (for products less than 1 kb) or 2% agarose (for products greater than 1 kb).

2.3. Preparation of clonal plasmids containing *CO2*ψ or authentic *CO2* mtDNA insert

CO2 PCR products were purified with a QIAquick PCR Purification Kit (Qiagen). This DNA was then ligated into pCR2.1 vectors containing an ampicillin resistance gene (Invitrogen, Carlsbad, CA). These ligation products were used to transform INVkF′ *E. coli* using the One Shot Kit (Invitrogen) and plated onto agar plates containing 100 μg/ml ampicillin. After overnight incubation at 37 °C individual colonies were selected and expanded in tubes containing EZMix LB broth (Sigma, St. Louis, MO) and 50 μg/ml ampicillin, miniprepped 18 h later using a QIAprep Spin Miniprep Kit (Qiagen), and checked for incorporation of the desired 611 bp insert by Eco R1 restriction digestion (New England Biolabs, Beverly, MA).

2.4. Analyses of nested PCR products and plasmids containing *CO2*ψ or authentic *CO2* mtDNA

Nested *CO2* PCR products were purified with a QIAquick PCR Purification Kit (Qiagen). Restriction fragment length polymorphism assays were performed on 750 ng of purified DNA using the restriction enzyme Bst N1 (New England Biolabs), electrophoresed on 2% agarose gels containing EtBr, and visualized under UV light. Plasmids containing *CO2* insert were also digested with the restriction enzyme Bst N1, electrophoresed on 2% agarose gels containing EtBr, and visualized under UV light.

DNA sequencing was performed on *CO2*-ligated pCR2.1 plasmids using the M13R and T7 primers. Sequence was determined with an Applied Biosystems Model 377 sequencer using the dideoxynucleotide chain termination technique.

2.5. Statistical analyses

Exact binomial upper 95% confidence limits for the proportion of one type of DNA product present when all of the selections were "other" types of DNA products were used to calculate maximum and minimum potential mtDNA copy numbers per cell (Rosner, 1995).

3. Results

We found human U251 glioma cells exposed to EtBr tolerated increasing amounts of this carcinogen. Table 1 shows the EtBr regimen used for mtDNA depletion of our U251 glioma cells. EtBr intercalates into mtDNA and interferes with its replication. As mtDNA depletion occurs cells become aerobically incompetent, but anaerobic survival is possible with uridine and pyruvate supplementation (King and Attardi, 1989). Most but not all cells became auxotrophic for pyruvate and uridine after several months, and only occasional reversion to aerobic competency was observed until 16 months in culture. Cell reversion during any particular selection trial prompted EtBr titration. We explored a range of EtBr concentrations with each successive titration, and in each case continued on with the highest concentration that did not markedly alter cell morphologically (Table 1). After 16 months of titrated EtBr exposure, cells selected completely in medium not supplemented with pyruvate and uridine.

At this point, we extracted genomic DNA and used PCR to screen for the presence of residual mtDNA. Primers that amplify mtDNA may also anneal to mtDNAψs or homologous mtDNA-like sequences that include serial pseudogenes, or numts, embedded in chromosomal DNA. We therefore used primers flanking but not including ($numt_{exclusive}$ primers) the ends of a previously reported numt sequence that corresponds to mtDNA positions 3914–9755 (Herrnstadt et al., 1999). Using primers that anneal to mtDNA upstream of mtDNA nucleotide 3914 and downstream of mtDNA nucleotide 9755 minimizes the likelihood of mtDNAψ amplification.

No amplification products were detected using the genomic DNA from the EtBr-treated cells and the $numt_{exclusive}$ primers. To confirm the integrity of this genomic DNA sample, PCR was performed using primers just internal to the borders ($numt_{inclusive}$ primers) of the Herrnstadt et al. numt, and this yielded a PCR product of the predicted size. As an additional positive control, we repeated the $numt_{exclusive}$ reaction with genomic DNA from non-EtBr treated U251 cells and obtained a product of the predicted size (Fig. 1). This indicates the primers and conditions of the $numt_{exclusive}$ reaction were functionally appropriate. Because PCR with the $numt_{exclusive}$ primers did not amplify a product from the EtBr-exposed U251 genomic DNA, this suggests that the EtBr-treated U251 cells constitute a ρ^0 line. To corroborate this result with "positive" data, we performed nested PCR reactions on the purified $numt_{inclusive}$ products of the EtBr-treated and untreated U251 cell genomic DNA samples, as well as from the purified $numt_{exclusive}$ product from the EtBr-untreated cells. The primers for the nested reaction were designed to anneal equally well to either the *CO2* gene of authentic mtDNA or to the *CO2* pseudogene contained within the Herrnstadt et al. numt. For each template analyzed, this PCR protocol resulted in bands of the expected size (Fig. 2).

Table 1
Ethidium bromide concentrations used to deplete U251 glioma cells of mtDNA

Incubation day	Ethidium bromide concentration (ng/ml)
1–74	25
75–104	50
105–114	100
115–389	600
390–424	800
425–590	1000

We sequenced the *CO2* amplicon produced by nested PCR of template originally generated through $numt_{inclusive}$ primer amplification of EtBr-treated genomic DNA. We compared the results of this to the known sequences of the authentic mtDNA *CO2* gene (Anderson et al., 1981) and the *CO2* pseudogene of the Hernstadt et al. numt (Hirano et al., 1997; Wallace et al., 1997; Davis and Parker, 1998; Herrnstadt et al., 1999). The differences between the authentic and pseudogenic *CO2* sequences are shown in Table 2. The Cambridge sequence (Anderson et al., 1981) contains a guanine at position 8152 of the mtDNA, and in several cell lines (including the U251 cell line) the nucleotide at the corresponding position on the *CO2* pseudogene is adenine. This adenine creates a unique Bst N1 restriction site that distinguishes wild-type mtDNA from the pseudogenic sequence.

We next digested our nested *CO2* products with Bst N1, and found no evidence of authentic mtDNA amplification in the EtBr-treated U251 cell genomic DNA (Fig. 3). These data suggest that with genomic DNA from the EtBr-treated cells, all PCR product produced with $numt_{inclusive}$ primers resulted from amplification of the Herrnstadt et al. numt.

To quantitatively analyze the nested amplicons generated with *CO2* primers, we ligated into plasmids the nested *CO2* PCR product generated using DNA template from $numt_{inclusive}$ primer amplification of EtBr-treated cell DNA. We also separately ligated into plasmids the nested *CO2* PCR product generated using DNA template from $numt_{inclusive}$ primer amplification of non-EtBr treated cell DNA, as well as *CO2* PCR product generated from $numt_{exclusive}$ primer amplification of non-EtBr treated cell DNA. We then used the plasmids containing insert from these three unique amplification protocols to transform *E. coli*. Transformants were grown as distinct colonies, which were expanded in broth prior to harvesting of the clonal plasmid DNA contained within. Plasmid DNA was digested with Bst N1.

We analyzed 62 colonies in which the *CO2* insert derived from amplification of template produced through $numt_{inclusive}$ amplification of EtBr-treated cell genomic DNA. In each plasmid clone analyzed, the restriction pattern was consistent with the presence of adenine at the position corresponding to nucleotide 8152 of the Cambridge sequence. None of these 62 clones appeared, therefore, to arise from amplification of genuine mtDNA.

For clones that were ultimately prepared from amplification of native U251 cell genomic DNA, we analyzed

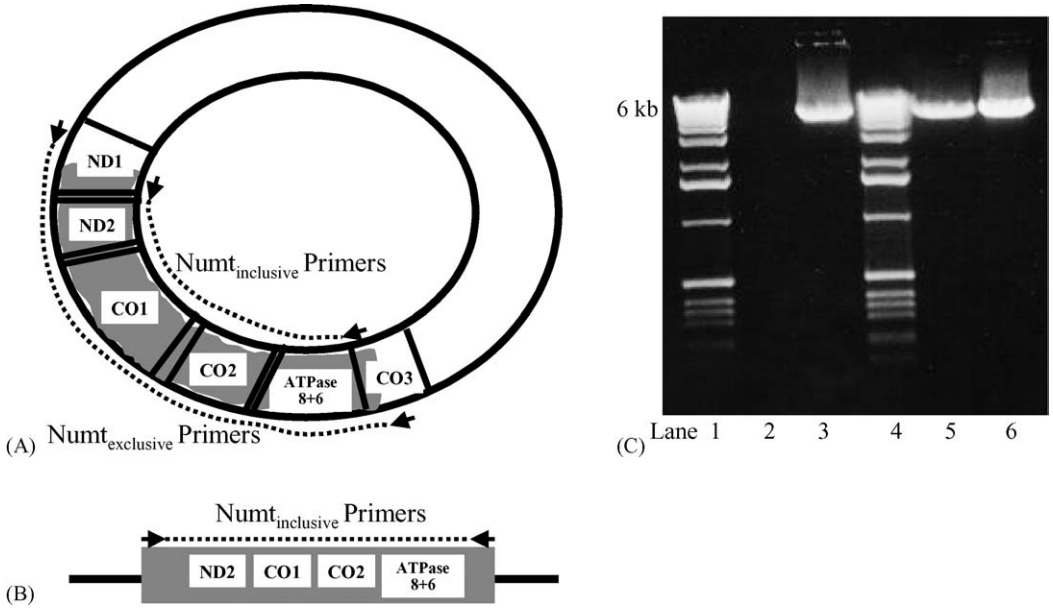

Fig. 1. Amplification of genomic DNA samples with primers inclusive ($numt_{inclusive}$) and exclusive ($numt_{exclusive}$) of a 5840 bp numt. (A) Schematic representation of the mtDNA genes that correspond to the 5840 numt. The numt contains part of ND1, CO3, and all mtDNA sequence in between. In the figure, it is indicated by the shaded pattern. Both $numt_{inclusive}$ and $numt_{exclusive}$ primers amplify mtDNA whose ends are either within the borders of the numt ($numt_{inclusive}$) or outside the borders of the numt ($numt_{exclusive}$). (B) $Numt_{inclusive}$ primers amplify the 5840 bp numt present in nuclear DNA, but $numt_{exclusive}$ primers do not produce any nuclear-based amplicons. (C) Actual amplification products using this PCR strategy. The first and fourth lanes contain a molecular weight marker. Amplification of genomic DNA extracted from EtBr-exposed U251 cells with $numt_{exclusive}$ primers yielded no detectable product (lane 2), while $numt_{exclusive}$ amplification of genomic DNA from untreated U251 cells did (lane 3). Use of the $numt_{inclusive}$ primers resulted in PCR product when both the treated (lane 5) and untreated (lane 6) genomic DNA was used as template.

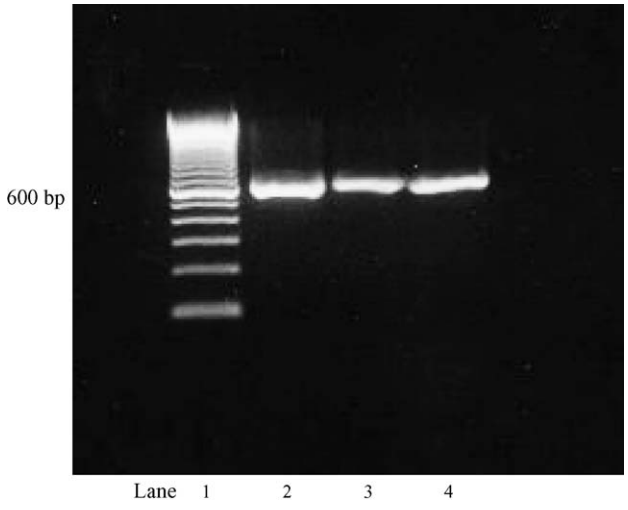

Fig. 2. Nested *CO2* PCR of DNA templates obtained via amplification of ethidium bromide-treated and untreated U251 cell genomic DNA with primers exclusive ($numt_{exclusive}$) and inclusive ($numt_{inclusive}$) of the 5840 bp numt. Lane 1 is a molecular weight marker. Lane 2 template was derived from $numt_{exclusive}$ primer amplification of EtBr-untreated U251 cell genomic DNA. Lanes 3 and 4 resulted from *CO2* primer amplification of the $numt_{inclusive}$ product of EtBr-treated and untreated cells, respectively.

Table 2
Analysis of a *CO2*-spanning mtDNA pseudogene in U251 cells: deviations from the Cambridge sequence between mtDNA nucleotides 7619–8230, as well as from *CO2* spanning pseudogene(s) from other mtDNA-depleted cell lines

Cambridge sequence deviations in the U251 pseudogene	Deviations from *CO2*-spanning pseudogenes in NT2, 143B-TK$^-$, or WAL2A-EB2 mtDNA-depleted cell lines
C7650T	–[a]
T7705C	–[a]
–[b]	A7771G in NT2 Cells
C7810T	–[a]
C7868T	Not present in all NT2 *CO2*-spanning pseudogene(s)
C7891T	–[a]
G7912A	–[a]
A8021G	–[a]
G8065A	–[a]
–[b]	C8080T in osteosarcoma cells
C8140T	–[a]
G8152A	Not present in osteosarcoma cells
–[b]	G8153A in osteosarcoma cells
T8167C	–[a]
C8197del	Not present in osteosarcoma cells
A8198del	Not present in osteosarcoma cells
C8203T	Not present in NT2 or osteosarcoma cells

[a] Indicates that no variability exists between the different cell lines at the specified position.
[b] Indicates that the U251 pseudogene matches Cambridge sequence.

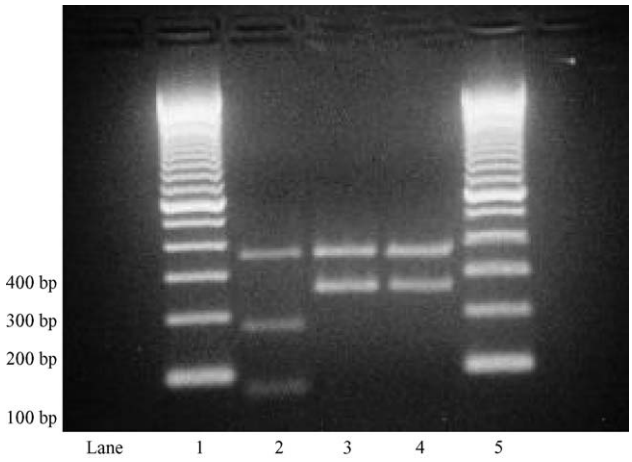

Fig. 3. Bst N1 digestion of nested *CO2* amplicons from Fig. 2. Lanes 1 and 5 contain a molecular weight marker that increases by 100 bp increments. In lane 2, the *CO2* generated from template produced via $numt_{inclusive}$ primer amplification of EtBr-treated cell genomic DNA cuts twice, yielding ~355, 177, and 79 bp fragments. This pattern is consistent with digestion of a previously described *CO2* pseudogene. In contrast, the *CO2* generated from template produced via $numt_{inclusive}$ primer amplification of EtBr-untreated cell genomic DNA (lane 3) cuts once, yielding 355 and 256 bp pieces. Digestion of *CO2* generated from template produced via $numt_{exclusive}$ primer amplification of EtBr-untreated cell genomic DNA (lane 4) similarly yields 355 and 256 bp pieces. The restriction pattern in lanes 3 and 4 is consistent with digestion of authentic mtDNA.

24 plasmid clones in which *CO2* was generated from template produced using $numt_{inclusive}$ primers, and 31 clones in which *CO2* was generated from template produced using $numt_{exclusive}$ primers. The Bst N1 restriction patterns for these clonal plasmid preparations were in each case consistent with the presence of guanine at the position corresponding to Cambridge nucleotide 8152 (Fig. 4). None of these clones, therefore, appeared to arise from mtDNAψ amplification.

We applied exact binomial upper 95% confidence limits to our clonal analysis data, and used these limits to calculate the maximum possible residual mtDNA copy number in the EtBr-treated cells. For example, we analyzed 62 clones containing *CO2* insert generated using template produced from $numt_{inclusive}$ primer amplification of EtBr-treated cell DNA, and all inserts appeared to contain *CO2* that derived from mtDNAψ. For 62 assessments, the exact binomial upper 95% confidence limit equals 0.0472. Therefore, with this number of samples we can say with 95% certainty that the number of authentic mtDNA amplicons present does not exceed 472 per 10,000 amplicon copies. Under this scenario, the smallest possible ratio of numt to authentic mtDNA-derived *CO2* amplicons is 9528:472, or 20.2 numt copies:1 mtDNA copy. Assuming an absence of preferential amplification and that two numt copies are present per cell, dividing the number of numt copies by 2 yields the maximum number of mtDNA copies per cell, which in this case is 10.1 cells:1 mtDNA copy, or slightly less than one copy of mtDNA per 10 cells. Table 3 displays the results of these calculations over a range of clone numbers.

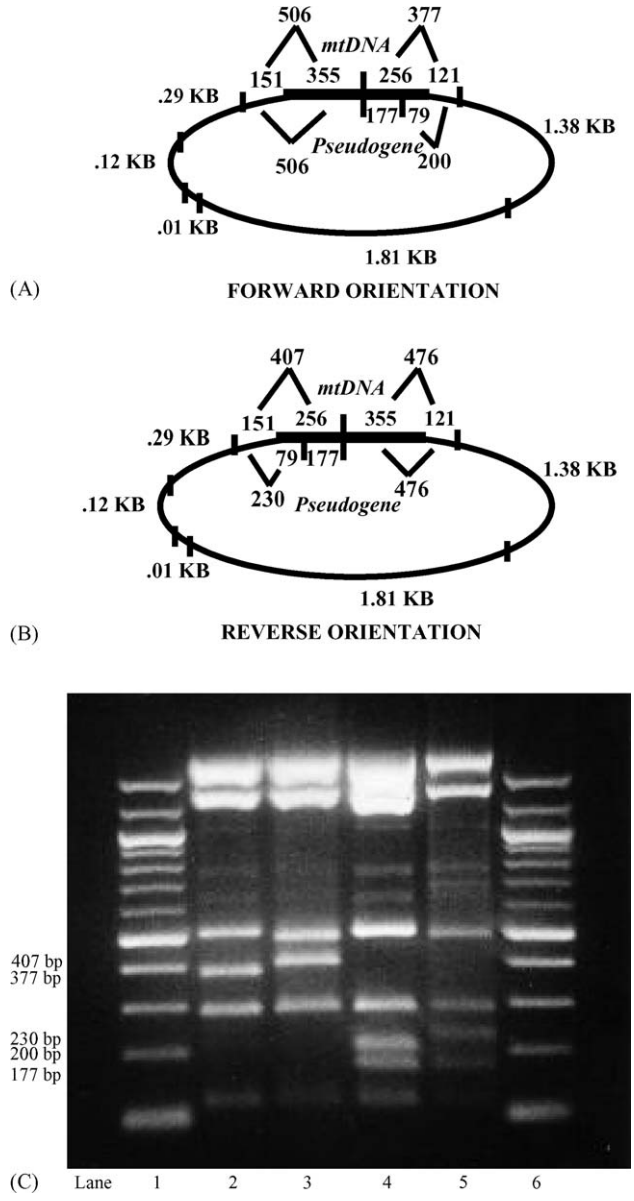

Fig. 4. Observed outcomes of Bst N1 restriction of clonal plasmids containing inserts of authentic or pseudogene *CO2* DNA. Plasmid insertions can occur with either a forward (A) or reverse (B) orientation. (A) and (B) indicate restriction sites when authentic mtDNA *CO2* or mtDNAψ *CO2* is inserted. Representative examples for these possibilities (forward vs. reverse orientation, authentic mtDNA vs. mtDNAψ *CO2* insertion) are shown in (C). By this method, it is possible to distinguish authentic mtDNA from mtDNAψ. In (C), lanes 1 and 6 contain a molecular weight marker showing 100 bp increments. The digested plasmid in lane 2 contained forward-inserted, genuine mtDNA (as is indicated by the presence of a 377 bp band). The digested plasmid in lane 3 contained reverse-inserted, genuine mtDNA (as is indicated by the presence of a 407 bp band). The digested plasmid in lane 4 contained forward-inserted *CO2*ψ (as is indicated by the digestion of the 377 bp piece seen in lane 2 into 200 and 177 bp pieces). The digested plasmid in lane 5 contained reverse-inserted *CO2*ψ (as is indicated by the digestion of the 407 bp piece seen in lane 3 into 230 and 177 bp pieces).

Table 3
Exact binomial upper 95% confidence limits for clonal analysis of plasmids containing *CO2* or the *CO2* pseudogene

Number of clones analyzed	All clones are pseudogene: maximum copies of mtDNA present (95% confidence limit)	All clones are mtDNA: minimum copies of mtDNA present (95% confidence limit)
10	<1 copy per cell	>5 copies per cell
20	<1 copy per 3 cells	>12 copies per cell
24	<1 copy per 3 cells	>15 copies per cell
30	<1 copy per 4 cells	>19 copies per cell
40	<1 copy per 6 cells	>25 copies per cell
50	<1 copy per 8 cells	>32 copies per cell
60	<1 copy per 9 cells	>39 copies per cell
62	<1 copy per 10 cells	>40 copies per cell
70	<1 copy per 11 cells	>45 copies per cell
80	<1 copy per 13 cells	>52 copies per cell
90	<1 copy per 14 cells	>59 copies per cell
100	<1 copy per 16 cells	>65 copies per cell

Bold values refer to the actual numbers performed in this analysis.

Alternatively, this technique can help determine the minimum number of mtDNA molecules extracted per cell. For the condition in which we analyzed *CO2* clones generated from template produced by $numt_{inclusive}$ primer amplification of EtBr-untreated U251 cell genomic DNA, exact binomial upper 95% confidence limits can specify the maximum number of non-mtDNA (or mtDNAψ) copies potentially generated during PCR. For 24 analyzed clones in which all clones were authentic mtDNA, the exact binomial 95% confidence upper limit value for the undetected DNA species (the pseudogene) is 0.1173. Thus, there should be no more than 1173 pseudogene-derived amplicons per 10,000 total amplicons. Assuming two copies of pseudogene reside within each cell, we can use the equation [((1 − upper limit of pseudogene copies)/upper limit of pseudogene copies) × 2] to calculate with 95% confidence the minimum number of mtDNA copies that were recovered per cell (Table 3). In this case, we can say with 95% confidence that when we prepared genomic DNA from the native U251 cells, at least 15.1 mtDNA copies per cell were extracted.

4. Discussion

With chronic exposure of immortalized cell lines to EtBr, it is possible to deplete endogenous mtDNA content below detectable levels and create ρ^0 cells. Of course, the sensitivity of residual mtDNA copy screening depends on the method of mtDNA detection used. Until now, the different mtDNA screening techniques utilized have relied upon interpretation of a negative result, such as the failure to amplify mtDNA segments using PCR or to hybridize an mtDNA probe on a blot.

Although nuclear mtDNAψs can complicate the study of authentic mtDNA, it is possible to exploit mtDNAψs for mtDNA depletion analysis. As mtDNA depletion proceeds, competitive amplification by primers that will anneal to either mtDNA or an mtDNAψ should increasingly favor production of the pseudogene. In principle, the ratio of mtDNAψ:mtDNA amplification should allow for an estimation of mtDNA copy number. In situations where no mtDNA amplification is apparent, it is possible to determine with statistical certainty a maximum possible number of residual mtDNA molecules in the cell culture.

Displacement of mtDNA sequences to nuclear chromosomes has occurred throughout evolution, both before and during the appearance of *homo sapiens* (Perna and Kocher, 1996). Since the sequence of the transferred mtDNA reflects the status of the authentic mtDNA present at the time of the transfer, these pseudogenic sequences remain as evolutionary "fossils" within the nucleus. Quantifying polymorphic divergence between modern mtDNA and a particular pseudogenic or numt sequence can help determine when the mtDNA in question moved from the mitochondria to the nucleus. In addition to varying by sequence, numts can vary by size and multiple permutations of a given mtDNA sequence may exist within chromosomes. These points are relevant because concomitant amplification of homologous numts may produce PCR products that differ at a restriction enzyme target sequence, which could confound the type of analysis we performed on our EtBr-treated U251 cells. Relying on amplification of long PCR fragments in this approach ideally should help reduce the chances of this occurring.

Aneuploidy or the presence of multiple mtDNAψ copies could alter the calculated values in Table 3, since the values provided in this chart assume two copies of mtDNAψ per cell. Regardless, this technique offers several advantages for the determination of ρ^0 status in cell lines intentionally depleted of mtDNA. It utilizes a positive result to confirm that mtDNA depletion occurred, allows one to statistically determine the extent of mtDNA depletion, and can pinpoint potential inadequacies in genomic DNA extraction methods.

This type of analysis is attractive in that it does not rely on interpretation of a negative result. While laborious, it can serve as an adjunct method for the determination of ρ^0 status in cell lines purposefully depleted of endogenous mtDNA. Our work in this regard does not address whether this approach will lead to production of "better" ρ^0 cell lines. In our experience, the ability of an mtDNA-depleted cell line to completely select and not revert at all in medium not supplemented with pyruvate and uridine provides the most practical indication of ρ^0 status. For investigators encountering ongoing reversion despite prolonged attempts to completely remove endogenous mtDNA from a cell line, this technique could nevertheless indicate how much residual mtDNA actually remains in their mtDNA-depleted line.

Acknowledgement

This work was funded by the National Institute of Aging.

References

Anderson S, Bankier AT, Barrell BG, de Bruijn MH, Coulson AR, et al. Sequence and organization of the human mitochondrial genome. Nature 1981;290:457–65.

Ashley N, Harris D, Poulton J. Detection of mitochondrial DNA depletion in living human cells using PicoGreen staining. Exp Cell Res 2005;303:432–46.

Bodnar AG, Cooper JM, Holt IJ, Leonard JV, Schapira AH. Nuclear complementation restores mtDNA levels in cultured cells from a patient with mtDNA depletion. Am J Hum Genet 1993;53:663–9.

Davis II JD, Parker Jr WD. Evidence that two reports of mtDNA cytochrome c oxidase "mutations" in Alzheimer's disease are based on nDNA pseudogenes of recent evolutionary origin. Biochem Biophys Res Commun 1998;244:877–83.

Desjardins P, de Muys JM, Morais R. An established avian fibroblast cell line without mitochondrial DNA. Somat Cell Mol Genet 1986;12:133–9.

Hayashi J, Ohta S, Kikuchi A, Takemitsu M, Goto Y, Nonaka I. Introduction of disease-related mitochondrial DNA deletions into HeLa cells lacking mitochondrial DNA results in mitochondrial dysfunction. Proc Natl Acad Sci USA 1991;88:10614–8.

Herrnstadt C, Clevenger W, Ghosh SS, Anderson C, Fahy E, Miller S, et al. A novel mitochondrial DNA-like sequence in the human nuclear genome. Genomics 1999;60:67–77.

Hirano M, Shtilbans A, Mayeux R, Davidson MM, DiMauro S, et al. Apparent mtDNA heteroplasmy in Alzheimer's disease patients and in normals due to PCR amplification of nucleus-embedded mtDNA pseudogenes. Proc Natl Acad Sci USA 1997;94:14894–9.

King MP, Attardi G. Human cells lacking mtDNA: repopulation with exogenous mitochondria by complementation. Science 1989;246:500–3.

King MP, Attardi G. Mitochondria-mediated transformation of human ρ^0 cells. In: Attardi GM, Chomyn A, editors. Mitochondrial biogenesis and genetics part B. Methods in enzymology, vol. 264; 1996a. p. 313–34.

King MP, Attardi G. Isolation of human cell lines lacking mitochondrial DNA. In: Attardi GM, Chomyn A, editors. Mitochondrial biogenesis and genetics part B. Methods in enzymology, vol. 264; 1996b. p. 304–13.

Martinus RD, Linnane AW, Nagley P. Growth of rho 0 human Namalwa cells lacking oxidative phosphorylation can be sustained by redox compounds potassium ferricyanide or coenzyme Q10 putatively acting through the plasma membrane oxidase. Biochem Mol Biol Int 1993;31:997–1005.

Miller SW, Trimmer PA, Parker Jr WD, Davis RE. Creation and characterization of mitochondrial DNA-depleted cell lines with "neuronal-like" properties. J Neurochem 1996;67:1897–907.

Perna NT, Kocher TD. Mitochondrial DNA: molecular fossils in the nucleus. Curr Biol 1996;6:128–9.

Rosner B. Fundamentals of biostatistics. 4th ed. New York: Duxbury Press; 1995.

Swerdlow RH, Parks JK, Cassarino DS, Maguire DJ, Maguire RS, Bennett Jr JP, et al. Cybrids in Alzheimer's disease: a cellular model of the disease? Neurology 1997;49:918–25.

Trounce I, Neill S, Wallace DC. Cytoplasmic transfer of the mtDNA nt 8993 T → G (ATP6) point mutation associated with Leigh syndrome into mtDNA-less cells demonstrates cosegregation with a decrease in state III respiration and ADP/O ratio. Proc Natl Acad Sci USA 1994;91:8334–8.

Wallace DC, Stugard C, Murdock D, Schurr T, Brown MD. Ancient mtDNA sequences in the human nuclear genome: a potential source of errors in identifying pathogenic mutations. Proc Natl Acad Sci USA 1997;94:14900–5.